

Article

Flocculation Behavior of Ultrafine Silica Particles in Acid Leaching Pulp by Nonionic Polymeric Flocculants

Bao Guo ^{1,*} , Xinlei Zhan ¹ , Kaixi Jiang ^{1,2,3,*}, Hongzhen Xie ² and Rongdong Deng ¹¹ Zijin School of Mining and Geology, Fuzhou University, Fuzhou 350108, China² State Key Laboratory of Comprehensive Utilization of Low Grade Refractory Gold Ores, Zijin Mining Group, Longyan 364200, China³ BGRIMM Technology Group, Beijing 100070, China

* Correspondence: guobao@fzu.edu.cn (B.G.); jiangkx@bgrimm.com (K.J.)

Abstract: Sedimentation of ultrafine silica particles that exist in acid leaching pulp and their separation from Pregnant Leach Solution largely determines the efficiency of a hydrometallurgical process utilizing copper oxide ore. Thickener on a larger scale can allow longer sedimentation, generating low overflow turbidity but high economic input. In this paper, the flocculation behavior of quartz particles in sulfuric acid solution using nonionic flocculants polyethylene oxide (PEO) and polyacrylamide (PAM), as well as ionic cofactor montmorillonite (MMT) and nonionic cofactor tannic acid (TA), were investigated, with the dynamic size of flocs and counts of fines being monitored using an in situ particle size measurement technique, namely the focused beam reflectance measurement (FBRM), under turbulent conditions. Attention was paid to variables affecting quartz flocculation properties from both physicochemical and hydrodynamic aspects such as shear intensity. The flocculation mechanism was investigated using zeta potential and dynamic light scattering measurements. It was found that the TA promotes the bridging flocculation of PEO-quartz by forming associative complexes with larger clusters in solution, while MMT electrostatically adsorbs on the quartz surface, enhancing its bridging with PAM. Low turbidity benefited from the higher shear resistance of the compact flocs structure provided by PEO/PEO + TA/PAM + MMT. Efficient solid–liquid separation was achieved by using the synergistic flocculation of small molecule cofactors and polymer flocculants.

Keywords: acid leaching; thickening; quartz; flocculation

Citation: Guo, B.; Zhan, X.; Jiang, K.; Xie, H.; Deng, R. Flocculation Behavior of Ultrafine Silica Particles in Acid Leaching Pulp by Nonionic Polymeric Flocculants. *Minerals* **2023**, *13*, 582. <https://doi.org/10.3390/min13040582>

Academic Editor: Kenneth N. Han

Received: 11 March 2023

Revised: 19 April 2023

Accepted: 19 April 2023

Published: 21 April 2023



Copyright: © 2023 by the authors. Licensee MDPI, Basel, Switzerland. This article is an open access article distributed under the terms and conditions of the Creative Commons Attribution (CC BY) license (<https://creativecommons.org/licenses/by/4.0/>).

1. Introduction

Solid–liquid separation in mineral processing/hydrometallurgy/wastewater treatment is frequently performed using gravity sedimentation. In the typical Solvent Extraction-Electrowinning (SX-EW) process utilizing oxidized copper ore, the Pregnant Leach Solution (PLS) is usually acquired by dense sedimentation of the acid leaching pulp, including thickening and the efficient Counter Current Decantation (CCD) [1]. However, the decomposition of silicate minerals introduces colloidal silica formed by the disordered condensation, seriously deteriorating solid–liquid separation. Kazadi found that the silica content of PLS can be minimized by controlling silica solubilization and polymerization, but the economic viability of the process still needs to be ascertained [2]. In addition, the easily argillized silicate minerals with low hardness, especially quartz, may generate a large fraction of ultrafine particles. Ultrafine particles settle slowly and incompletely, and their entrainment into the overflow can lead to the formation of third-phase crud during solvent extraction [3,4]. Therefore, polymeric flocculants with high molecule weight, typically polyacrylamide, are used to aggregate small, suspended particles into larger flocs for more efficient sedimentation. The electrostatic forces between particles are responsible mostly for repulsion and, consequently, suspension. Aggregation of fine particles can be achieved by neutralizing the electrical charge of the interacting particles, which is coagulation, in addition to bridging the particles by nonionic polymeric flocculants, which is flocculation [5–7].

High-molecule-weight flocculants can be extremely effective in promoting floc growth in previously stabilized suspensions [8]. Ionic polymeric flocculants play the dual roles of coagulation and flocculation.

In acid leaching pulp, most of the minerals' particle surfaces are positively charged as a result of protonation. By adding coagulants to the isoelectric point, usually by adjusting the solution pH, the suspension system can be destabilized. Zinc hydrometallurgy benefits from the neutralization of acid leaching pulp to pH 5.0~5.2, where coagulation occurs between silica particles and iron hydroxide particles, the solution purification method before the electrolysis process [9,10]. By using the "neutralization-coagulation" strategy, researchers attempted to remove the crud silica/clay particles in a raffinate solution, which is recirculated to the leaching process in copper hydrometallurgy [11]. However, the problem of fine particles dragged from the feed still exists. Solvent extraction as a downstream circuit operation in acidic media prevents neutralization afterwards. Cationic surfactant cetyl trimethyl ammonium bromide addition could disturb the stability of kaolinite suspensions to some extent in copper hydrometallurgy conditions, as a result of surface charge neutralization [12]. Nonionic TX 100 surfactants were also found to improve the settling rates of kaolinite in combination with nonionic polyacrylamide due to the mutual interaction of polymer and surfactants [13]. Polystyrene sulfonate was also suitable for charge neutralizing in polyethylene-oxide-induced flocculation [14]. However, the application of surfactants usually requires either excessive dosage levels or tedious operation to avoid overcharging.

In this paper, we report an operative combination of high-molecular-weight polymer flocculants and low-molecular-weight cofactors to improve the sedimentation of acid leaching pulp. The small molecules not only play the role of coagulants, but also enhance the functionality of flocculants, borrowing the idea of the flocculation cofactor that has been extensively investigated in the papermaking industry [15,16]. The performance of nonionic flocculants polyethylene oxide (PEO) and polyacrylamide (PAM), ionic cofactors montmorillonite (MMT), and tannic acid (TA) were studied in quartz–sulfuric acid system, and different flocculation models were proposed.

2. Experimental

2.1. Materials

Quartz is typically a major component within residues from the digestion of copper oxide feeds. Herein, quartz was used as a synthetic substrate to represent leaching residue in this work, the source varying in terms of the particle size. One source of quartz sample was the product of closed-circuit grinding, and its particle size distribution was measured using a Malvern Mastersizer 2000, as shown in Figure 1a. The ground sample had a D_{90} of 54.690 μm and D_{50} of 19.588 μm , while 31.98% of the mass was attributed to fine particles ($\leq 10 \mu\text{m}$). The deviation from the Normal Distribution indicated that significant argillization had occurred, raising a problem for solid–liquid separation. As this study sought to emphasize the impact of the flocculation efficiency of fine particles, a quartz sample source of 2000 mesh was also used. The X-ray diffraction in Figure 1b confirmed the crystalline phase of the quartz samples.

The molecular structures of nonionic flocculants polyethylene oxide (PEO, from Macklin) and polyacrylamide (PAM, commercially provided as 6003s from SNF) as well as cofactor tannic acid (TA, from Aladdin) are shown in Figure 2. Their molecular weights are listed in Table 1. Concentrated (0.10 wt.%) stock solutions were prepared no more than 7 days prior to use: Powder flocculant (0.2 g) was added slowly into the vortex of deionized water (200 mL), with the stirring speed at 600 rpm for 5 min. Afterwards, the stirring speed was reduced to 250 rpm and maintained for another 12 h. The stock solutions were sealed in a glass beaker using parafilm at room temperature before use. The dosage of flocculants added into the quartz slurry is expressed as g/t (grams of flocculant per ton of quartz solids), and it varies from 10 to 100 g/t.

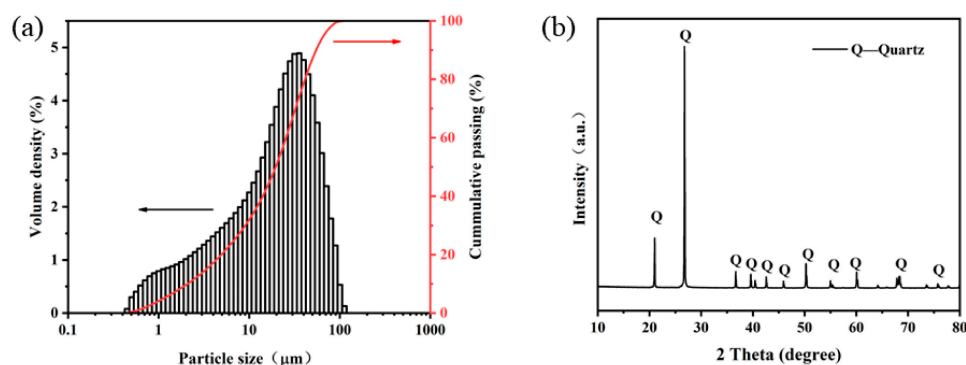


Figure 1. (a) Particle Size Distribution (PSD); (b) XRD pattern of quartz sample.

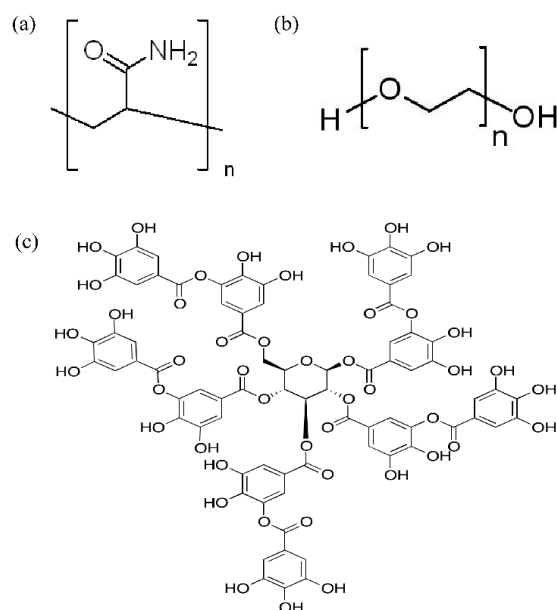


Figure 2. Molecule structure: (a) PAM; (b) PEO; (c) TA.

Table 1. Flocculants/Cofactors used in this study.

	Molecular Weight, g/mol	Type
PEO	7 million	Powder
PAM	10~12 million	Powder
MMT	low	Powder
TA	1701.20	Powder

Montmorillonite (MMT) is a nanolayered phyllosilicate mineral that consists of two O-Si-O tetrahedral sheets sandwiching one O-Al(Mg)-O octahedral sheet, as shown in Figure 3. Isomorphous substitutions always exist. For example, Si^{4+} in the tetrahedral sheet can be replaced by Al^{3+} ; Al^{3+} in the octahedral sheet can be replaced by Mg^{2+} [17]. Due to such an isomorphous substitution, the MMT nanolayer exhibits inherent negative charges, which can be compensated for by cations (Na^+ , Ca^{2+}) in the interlayer space [18,19]. It is noted that these negative charges are permanent, differing from carboxylic acid which cannot be dissociated below its pKa. In particular, the van der Waals force and electrostatic force holding the MMT nanolayers together can be overcome by certain methods. For example, MMT particles disassembled in aqueous dispersion, leading to reduced particle size. Ultimately, the fine MMT particles can be exfoliated to an individual nanolayer [20]. Figure 4a shows the PSD of the MMT sample. It was found that the water dispersed sample had a D_{90} of 4.521 μm and D_{50} of 0.842 μm , indicating the presence of single or multiple

nanolayers. Larger particles may be attributed to MMT aggregates or the presence of impurities, including quartz and albite. As shown in the XRD pattern in Figure 4b, the MMT sample had a $d_{(001)}$ -spacing of 14.579 Å ($2\theta = 6.057^\circ$), which is a mixture of Ca^{2+} -MMT and Na^+ -MMT [21]. The MMT slurry was stirred for at least 12 h prior to use for ample hydration and exfoliation.

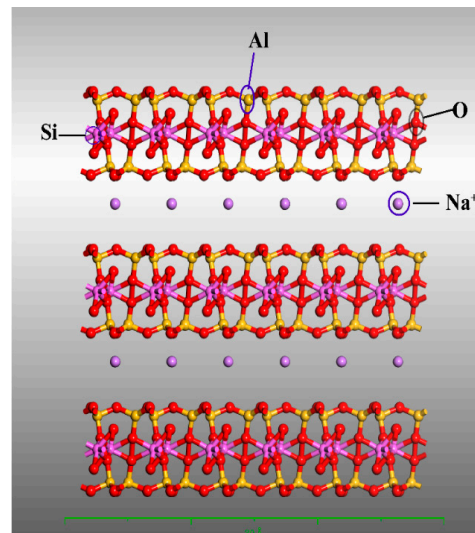


Figure 3. Crystal structure of montmorillonite.

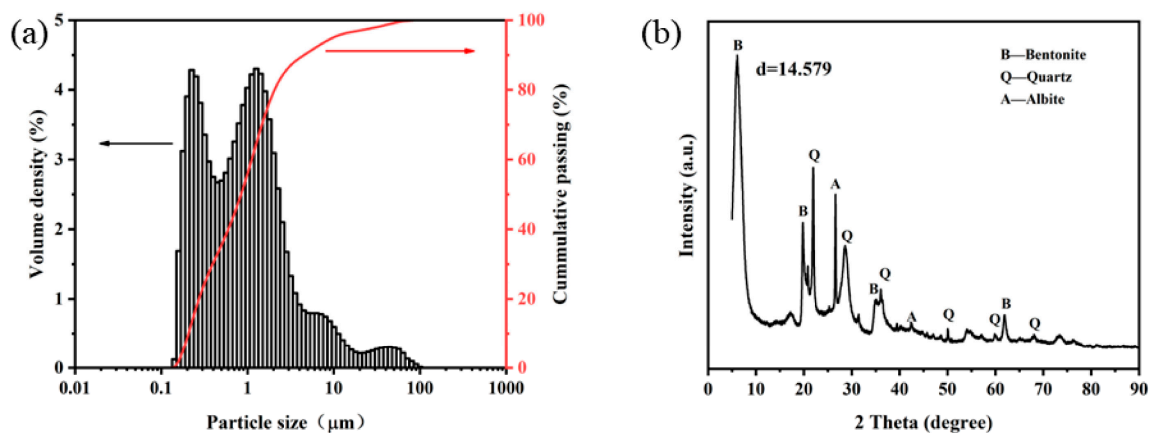


Figure 4. (a) Particle size distribution; (b) XRD pattern of montmorillonite sample.

2.2. Flocculation Sedimentation Tests

Slurries were prepared by adding a known amount of the quartz sample to 100 mL of water in a 150 mL glass beaker (diameter 5.8 cm, height 8.8 cm) fitted with a C50 stir bar (diameter 8 mm, length 5 cm). The pH of the slurry was adjusted to 1.5 using sulfuric acid, then it was preconditioned at a high mixing intensity (600 rpm) for 15 min. In this work, 10 g of the closed-circuit ground 200-mesh quartz sample was added to make a 10 wt.% slurry, while 1 g of the 2000-mesh quartz sample was added to make a 1 wt.% slurry.

After the high intensity mixing, the stirring speed was decreased to 200 rpm prior to the addition of the flocculants, then stirring was continued for 1 min. Where applicable, cofactors were added 1 min prior to the addition of flocculants at a constant stirring rate. The flocculated slurry was then poured into a 100 mL measuring cylinder and settled naturally. Settling was allowed to proceed for various selected durations, then 2 mL of supernatant was carefully syringed 1 cm underneath the water surface. The sampled supernatant was diluted where necessary for the turbidity measurement (LEI-CI WZB-175).

2.3. FBRM Measurement

The particle and aggregate size at different stages of flocculation were examined *in situ* using the FBRM, the principle of which has been described previously by Fawell, P.D. et al. [22,23]. All FBRM measurements were carried out using a Mettler Toledo G400 field unit fitted with a laboratory probe. The probe has a flat sapphire window of 9.5 mm diameter located at the tip of the stainless-steel body (136/70 mm long, 14/9.5 mm diameter).

A polytetrafluoroethylene container (internal diameter 7.0 cm, height 7 cm) was custom built to accommodate the FBRM probe in a horizontal position near the inner wall of the container, 1 cm above the bottom and away from the C50 stir bar. The probe had a 45° angle to the tangent direction of the flow speed to avoid flocs adhering to the sapphire window, as shown in Figure 5. Such configuration of the probe tip not only ensures good sample presentation but also allows slow-stirred slurry to be measured. This is due to excessively large flocs settling down to the bottom of the container easily during slow stirring; however, obvious breakage of flocs occurs once sped up.

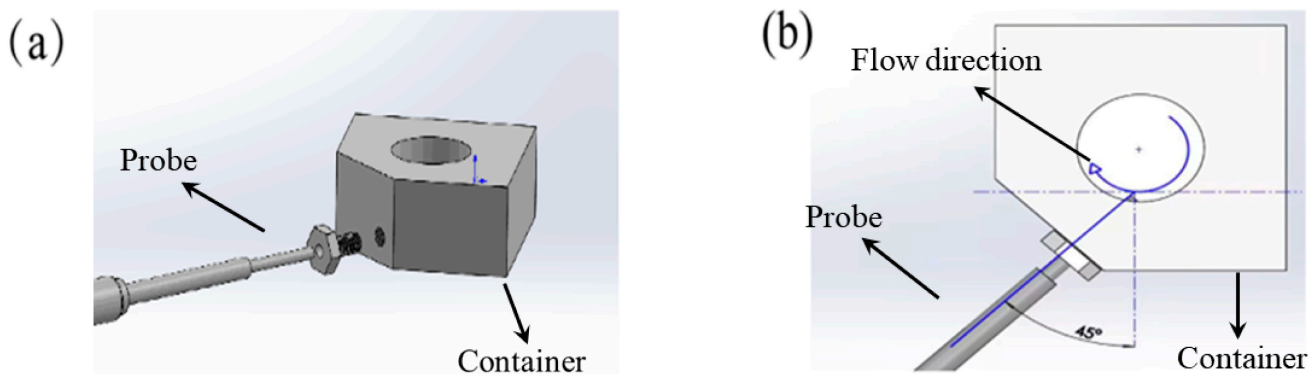


Figure 5. Configuration of custom-built container to accommodate the FBRM probe: (a) stereogram; (b) vertical view.

The FBRM data was processed and analyzed using Version 4.4 acquisition software. It was continuously scanned with a 2 s duration over the full range of chord lengths (1 to 4000 μm). Chord Lengths Distributions are expressed as line graphs for simplicity. Both unweighted and square-weighted chord lengths were acquired using the software. The unweighted chord length distribution is number-sensitive, providing an implication for the fine particles that are suspended in the slurry. Square-weighted chord length distribution represents the volumetric and mass contribution of the large flocs in the slurry.

Primary mode and macro mode measure flocs in a different way. The primary mode is suitable for detecting the suspended fine particles, while the response of macro mode is too slow to capture fine particles. With respect to the primary mode, each section of the porous large floc is considered as a single chord length, while the slower macro response tends to detect each floc as a single particle with a single chord length. When we are aiming to monitor the growth and breakage of flocs (flocculation kinetics), the macro mode with volumetric weightings is recommended. Alternatively, unweighted chord length distributions in primary mode are preferred if we need to measure the counts of fine particles [24].

2.4. Zeta Potential and Effective Diameter Measurements

The zeta potential of quartz dispersions was measured using a NanoPlus3 (Micromeritics Instrument, Norcross, GA, USA). The quartz dispersion was prepared by adding 5000-mesh fine particles to 10^{-3} mol/L KNO_3 solution at a solid concentration of 0.5 mg/mL, sonicating for 30 min, and allowing it to stand for 24 h. Afterwards, the supernatant was transferred into a disposable cell for zeta potential measurement. The cell was kept at 25 °C and equilibrated for 120 s prior to measurement. The pH of dispersion was regulated

by adding a suitable amount of 10^{-1} M NaOH or HNO₃; a desired amount of MMT was added, followed by conditioning for 30 min.

The effective diameters of the flocculant's molecule and their associated complexes in aqueous solution were determined using a Malvern ZS90. The effective diameter is the hydrodynamic diameter of a polymer molecule conformation. For a polydisperse system, the effective diameter measured is a value calculated from the averaged intensity of the scattered light for each particle. The 0.1 wt.% PEO/PAM stock solutions were prepared, as described above, 12 h before being added into the cuvette. The 0.1 wt.% TA was mixed with PEO stock solution and stirred at 200 rpm for 1 min before measurement.

3. Results and Discussion

3.1. Flocculation Sedimentation

The settling behaviors of quartz slurry were investigated to examine the flocculation efficiency of the proposed polymers-cofactors system. The supernatant turbidity of 10 wt.% -200-mesh quartz slurry during sedimentation is shown in Figure 6. These sedimentation curves can be described using the exponential decay of turbidity as a function of time. The use of PEO at a dosage of 10~100 g/t settles significantly faster, with 10-min turbidity reduced to 94.4 NTU (100 g/t), compared to 834 NTU (100 g/t) at the same dose of PAM. Low turbidity indicated a better clarity of the supernatant, containing a smaller number of suspended particles. In the simulated acidic leaching pulp, PEO was proved to be more efficient to flocculate quartz particles. On the other hand, PAM might be good at accelerating settling rate, but it was not capable of controlling the turbidity of the supernatant, even with an excessive dosage.

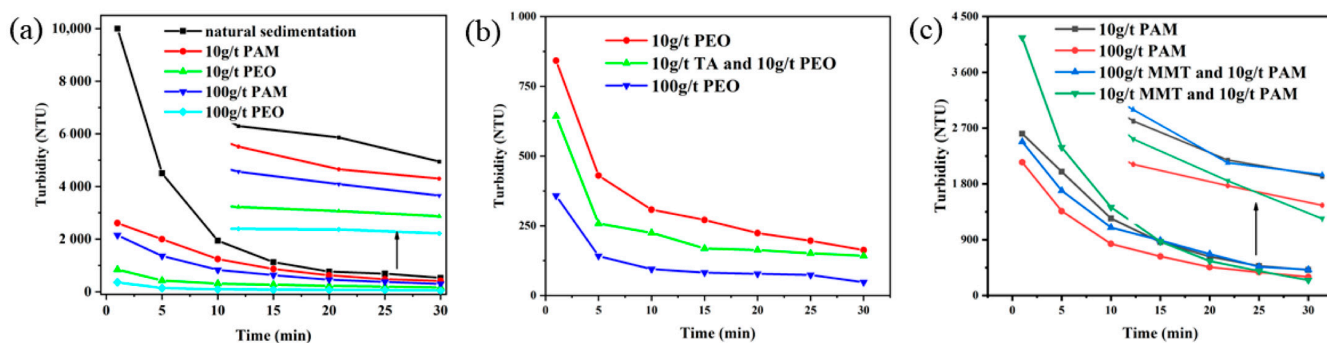


Figure 6. Supernatant turbidity of 10 wt.% -200-mesh quartz slurry during a 30-min sedimentation: (a) high molecule flocculants; (b) PEO and cofactor; (c) PAM and cofactor.

It is seen from Figure 6b that the combination use of TA-PEO gave a clearer supernatant with further decreased turbidity compared to that of PEO alone. It suggested that TA could promote the formation of larger quartz flocs using PEO, causing faster settling rates and entrapping more fine suspended particles. Such a synergistic effect was, however, not found for the combination use of MMT-PAM. The turbidity was even higher after the addition of MMT into the PAM system, as seen from Figure 6c. These extra suspended fine particles were probably contributed by the slow settling MMT nanolayers.

The settling behaviors of 1.0 wt.% 2000-mesh quartz slurry were also studied to examine the flocculation efficiency of fine particles, mimicking the clarification of turbid thickener overflow. The results in Figure 7a show that PEO was still very effective in flocculating fine particles. A lower supernatant turbidity can be obtained with only 10 g/t PEO than its PAM counterpart at the same dosage. The effect of TA addition to PEO was identical to that of a -200-mesh quartz system, significantly decreasing the turbidity. For example, the addition of 10 g/t TA to 10 g/t PEO exhibited lower turbidity (470 NTU at 5-min sedimentation). It is noted that settling accelerated after the first several minutes for PEO and PEO-TA systems, indicating a longer incubation time for floc formation than other flocculants. It is seen from Figure 7c that adding any amount of MMT did not accelerate

the settling of fine quartz particles based on 10 g/t PAM. On the other hand, the addition of 10 g/t MMT prior to 100 g/t PAM dramatically accelerated settling with much lower turbidity of the supernatant (402 NTU at 10-min sedimentation). The possibility of failure in the PAM-MMT in 200-mesh quartz slurry because most of the MMT was consumed by coarse particles which settled easily.

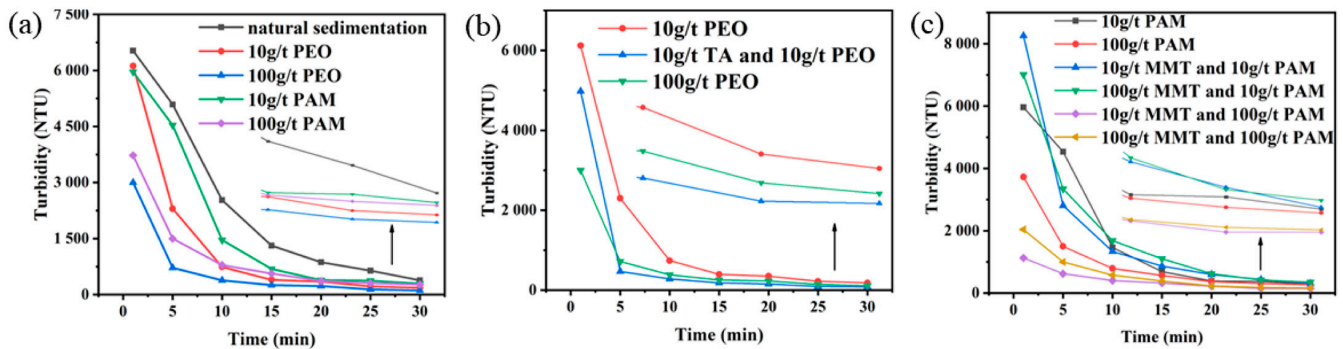


Figure 7. Supernatant turbidity of 1 wt.% -2000-mesh quartz slurry during a 30-min sedimentation: (a) high molecule flocculants; (b) PEO and cofactor; (c) PAM and cofactor.

3.2. Flocs Formation and Breakage

Figure 8 shows the mean particle size (MPS) and particle size distribution (square weighted, macro mode) evolution as a function of time for 10 wt.% 200-mesh quartz slurry at 400 rpm. As can be seen, a dramatic increase of MPS was observed upon the addition of flocculants (100 g/t PEO at 90 s). During the flocculation stage (90~106 s), the flocs rapidly grew to reach a maximum size. The maximum MPS was about 230 μm under the tested condition. The floc size soon experienced a continuous decrease upon exposure to a longer reaction time at a constant shear rate. At the end of the measured period (300 s), the mean floc size decreased to ~118 μm, not far from its original value without any addition of flocculants.

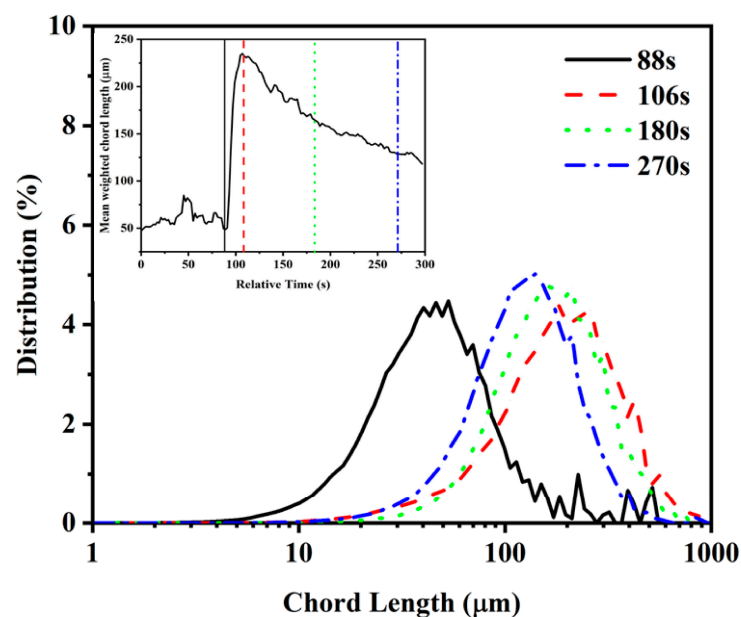


Figure 8. The trend of Mean Particle Size and PSD (square weighted, macro mode) as a function of stirring time: 100 g/t PEO, 400 rpm.

Figure 9 demonstrates the FBRM results of different flocculants/cofactors systems that used quartz flocculation at a stirring speed of 200 rpm. The cofactors (TA/MMT) were

added 60 s prior to flocculant (PEO/PAM) additions, and all reagents were used at a dosage of 100 g/t. As can be seen, the particle size did not change in the period from 0 s to 90 s, indicating that cofactors alone were incapable of flocculating quartz particles without the presence of high molecule weight flocculants.

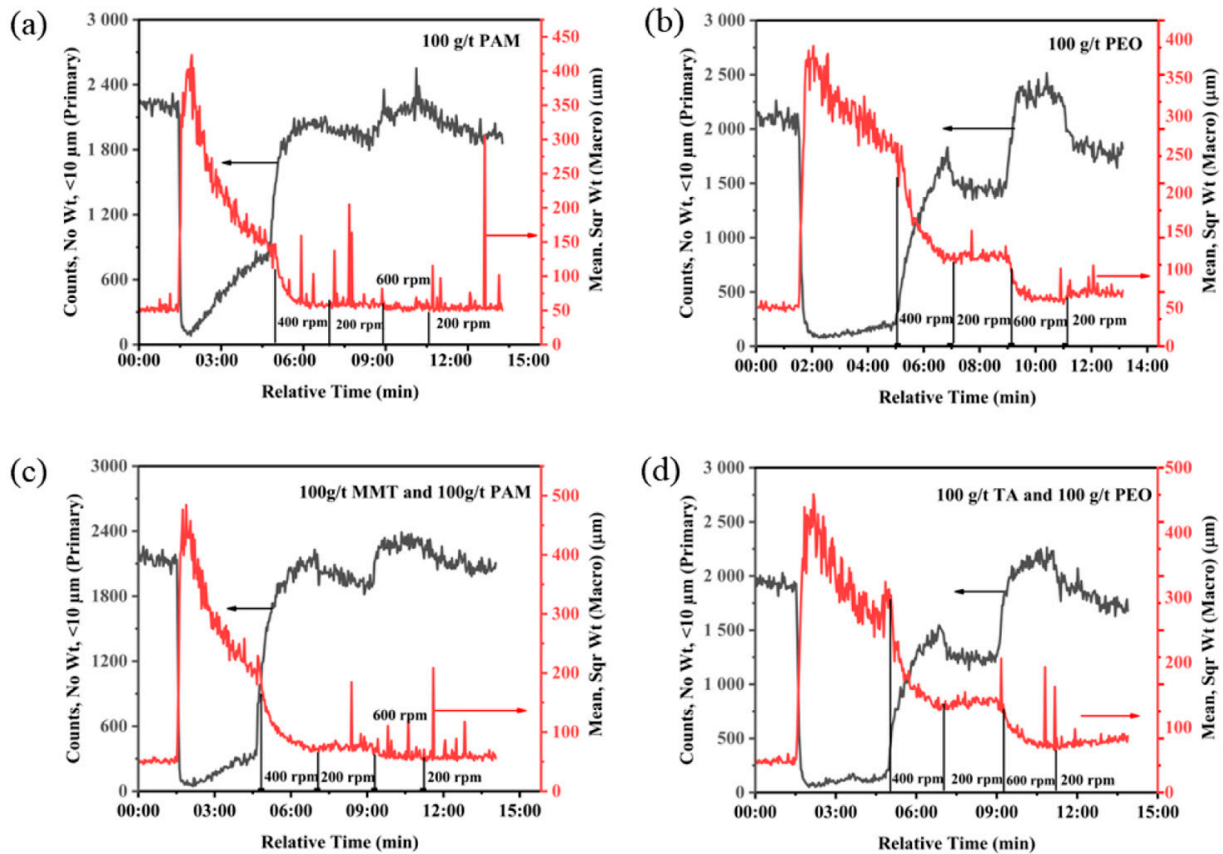


Figure 9. The trend of Mean Particle Size (MPS) (square weighted, macro mode) and Counts of Fine Particles (CFP) ($\leq 10 \mu\text{m}$, no weighted, primary mode) as a function of stirring time: initially 200 rpm and accelerated afterwards: (a) PAM; (b) PEO; (c) PAM-MMT; (d) PEO-TA.

The maximum floc size reached $\sim 410 \mu\text{m}$ by adding PAM, which was slightly larger than that formed by PEO. Upon the addition of MMT, the MPS increased sharply to more than $450 \mu\text{m}$, enhancing the flocculation of quartz particles by PAM. Additionally, the addition of TA leads to larger floc size as a result of the synergistic effect between TA and PEO. The floc size in all situations then experienced a continuous decrease upon exposure to a longer reaction time, and the slope of the decrease was calculated and listed in Table 2. It was found that PEO and PEO-TA systems exhibit a much smaller slope (absolute value) compared to their PAM and PAM-MMT counterparts. It means that PEO and PEO-TA systems experienced a weaker degree of aggregate rupture during longer reaction times after the peak magnitude.

Table 2. Slopes of MPS decrease and CFP increase.

		PAM	PEO	PAM-MMT	PEO-TA
200 rpm	MPS	−2.08	−0.76	−2.25	−1.27
	CFP	4.92	0.45	1.42	0.49
400 rpm	MPS	−1.98	−0.87	−2.09	−0.59
	CFP	13.66	7.89	14.13	7.31

Counts of Fine Particles (CFP) ($\leq 10 \mu\text{m}$, no weighted, primary mode) were calculated using FBRM software and the results for quartz flocculation at 200 rpm were also presented in Figure 9. Particles finer than $10 \mu\text{m}$ contributed to most of the turbidity after settling and their counts sharply decreased to a very low level upon the addition of any type of flocculant (from more than 2000 to less than 200). However, the CFP soon increased to much higher values in the case of PAM, as shown in Figure 9a. The addition of MMT can be helpful to keep the low number of fine particles for PAM with only a small increase after 2~3 min of shear action. During conditioning with PEO and PEO-TA at 200 rpm, the CFP were almost constant at a very low level, reflecting the stability of flocs. For comparison, the slope of the CFP increase was also calculated and listed in Table 2.

The results of the FBRM corresponded well with flocculation behaviors based on turbidity measurement. It indicated that PEO-TA and PAM-MMT acted synergistically to create more stable flocs from the quartz suspension with high resistance to floc breakage when subject to shear force. It is seen from Figure 9 that the flocs formed quickly but broke quickly under the use of PAM alone. In practice, the mixing reaction time of slurry and PAM in the feed pipe and feed well can last longer than 1 min, resulting in significantly broken flocs. The PEO and its combination with TA, as well as the PAM-MMT combination, help the flocculation of quartz slurry due to their higher shear resistance.

In addition to the molecule type and their combination, the flocculation process can also be affected by hydrodynamics, especially turbulence intensity. Figure 9 also shows full profiles for quartz flocculation switching to a higher stirring rate after the initial 200 rpm. Generally, higher shear rates (400 rpm and 600 rpm) can give a faster rate of floc breakage, together with the sudden release of fine particles. Such degradation of flocs at high turbulence occurs following such an order: PAM > PAM-MMT > PEO > PEO-TA.

When the lower shear rate (200 rpm) was restored, the floc size remained unchanged. This indicated that nonionic PAM/PEO-induced flocculation was irreversible upon high shear, and the flocs did not regrow after breakage. After resuming the initial lower shear rate, the CFP slightly reduced. Reflocculation may occur but not in the form of floc size regrow.

This was consistent with expectations that high-weight-molecule-flocculating solid particles can be effectively deactivated as a result of breakage and unable to bridge these particles again. These results shed light on the critical differences between coagulation and flocculation [25]. Aggregates are produced as a result of charge neutralization for coagulation, and a reduction in shear intensity usually leads to the regrowth of aggregate while a new equilibrium can be reestablished. In contrast, flocs formed by polymer-bridging does not lead to a new equilibrium once the bridging ruptures, and the dismantlement of fine particles is irreversible without any additional flocculant dosage.

Applying a cycled shear scheme as shown in Figure 9 is a good tactic to study the floc strength and floc reversibility under different turbulent conditions [26,27]. The above results indicate that only fine flocs can be partially reflocculated after breakage. In order to calculate the MPS decrease slope and CFP increase slope at higher shear strength, FBRM test work was conducted for freshly prepared quartz slurry at a constant stirring speed of 400 rpm, and the results are shown in Figure 10. The corresponding slopes in Table 2 further indicate that PEO and its combination with TA outperformed PAM and PAM-MMT, in terms of floc strength. However, it is better to avoid either intense turbulent condition or long reaction time. Judicious feed well optimization allows aggregate growth to take place under the milder shear experienced immediately below the feed well exit. The implementation of the FBRM online particle size measurement allows design options or flocculant addition points to be identified that produce the optimal residence time and flocculation response [28,29].

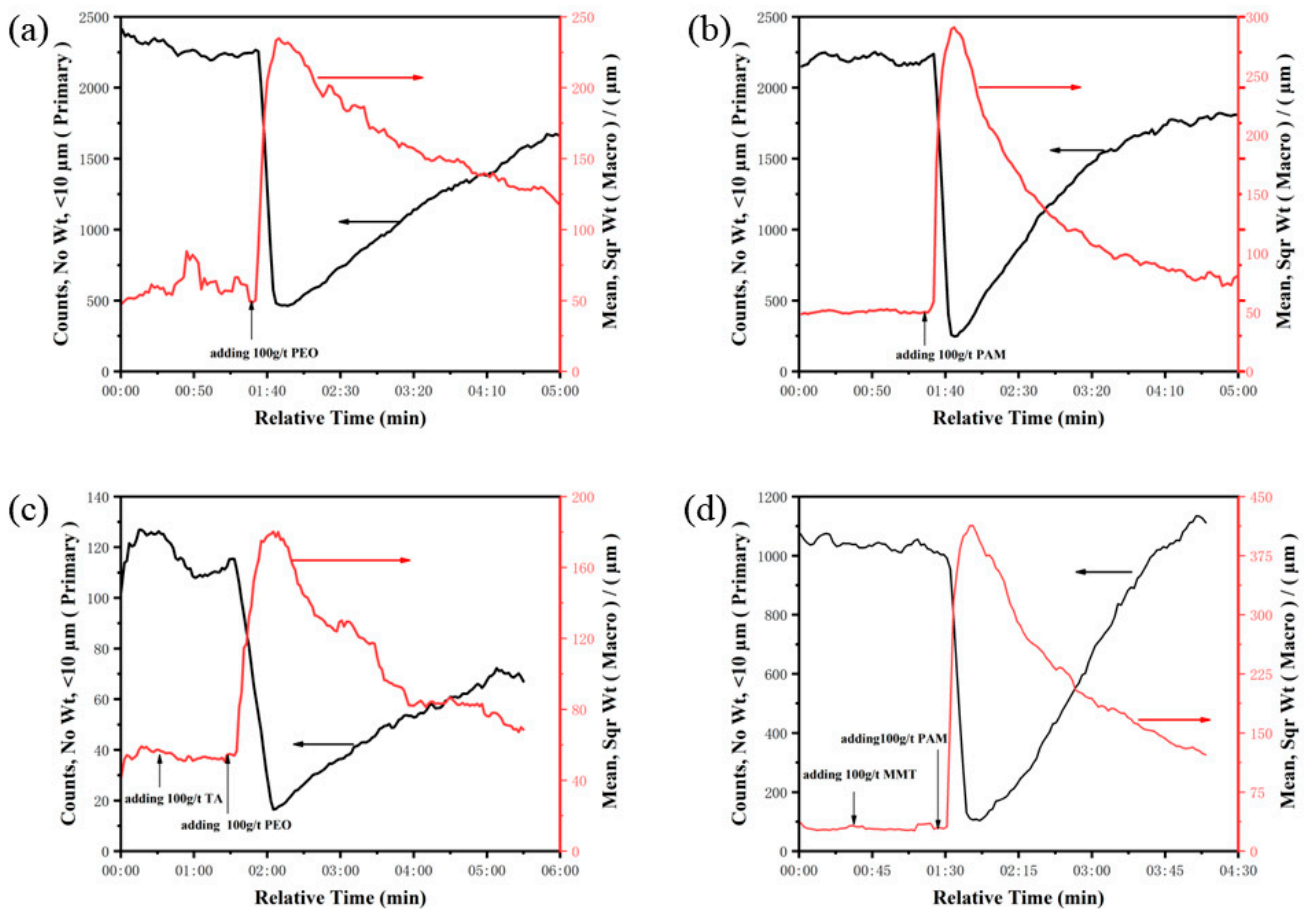


Figure 10. The trend of Mean Particle Size (square weighted, macro mode) and Counts of Fine Particles ($\leq 10 \mu\text{m}$, no weighted, primary mode) as a function of stirring time: 400 rpm: (a) PEO; (b) PAM; (c) PEO-TA; (d) PAM-MMT.

3.3. Mechanisms of Flocculation

To achieve the synergistic function of the flocculants/cofactors dual reagents system in quartz flocculation, several pathways were possible. One way is that cofactors adsorb onto the quartz surface acting as the bridge and facilitating the adsorption of flocculants. Another possible pathway is that cofactors act as coagulant, neutralizing surface charge.

Zeta potential is an important parameter of the stability of colloidal suspensions. Figure 11 shows the zeta potential of quartz at pH 1.5 and pH 7, respectively. Quartz particles were negatively charged at pH 7 (-36.95 mV), but positively charged at pH 1.5 (11.04 mV). It has been reported that the point of zero charge (PZC) for quartz suspension is pH 2, below which silanol groups ($-\text{Si}-\text{O}^-$) are dominant, rendering its surface negatively charged, while these silanol groups can be protonated at acidic pH, resulting in a positively charged surface [11,26]. It is generally accepted that the stability of colloidal dispersion depends on surface charge, with zeta potential of $\leq \pm 10 \text{ mV}$ corresponding to unstable dispersion, and $\geq \pm 30 \text{ mV}$ corresponding to a stable dispersion as a result of the electrostatic repulsion [6]. The present quartz suspension should be relatively unstable without flocculants; however, it naturally settles slowly, which is still inadequate for high throughput thickening performance.

A reduction in the magnitude of the zeta potential was observed with the increasing MMT concentration in acidic conditions (2.74 mV for 10 g/t and -0.63 mV for 100 g/t). The absence of electrostatic repulsion would cause the system to aggregate under van der Waals attractive forces. The quartz suspension can then be destabilized to some extent by MMT adsorption, due to a reduction in the magnitude of the surface charge.

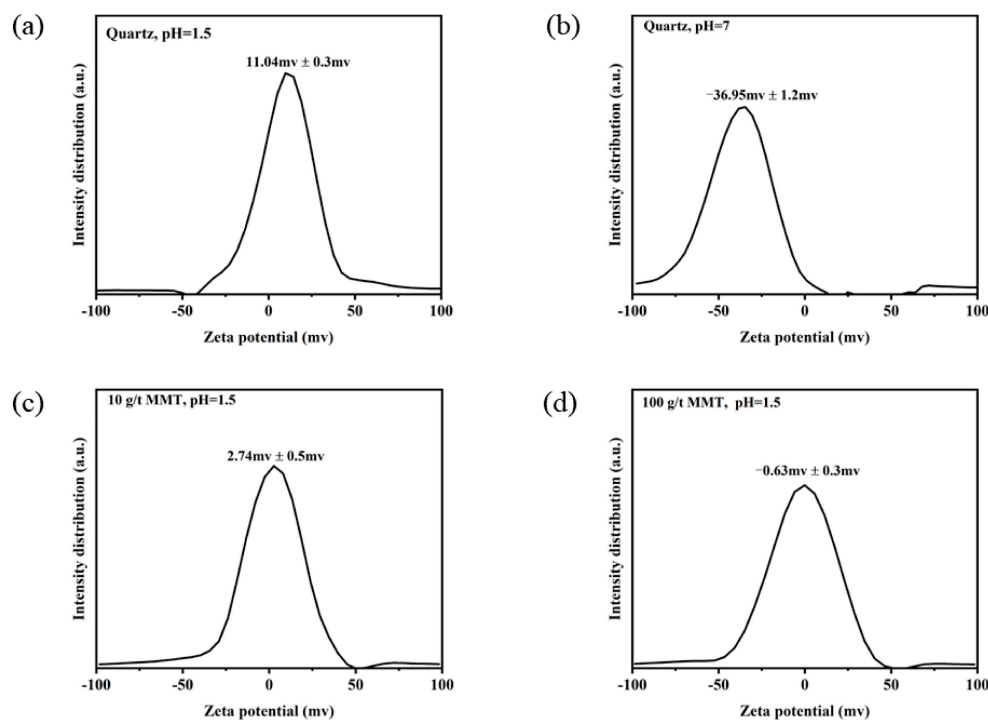


Figure 11. The zeta potential of quartz suspension: (a) pH1.5; (b) pH7; (c) pH1.5 with 10g/t MMT; (d) pH1.5 with 100g/t MMT.

The addition of MMT significantly improved the flocculation efficiency by PAM. However, the authors believed that coagulation caused by MMT's charge neutralization might not be the main contributor for an improvement. Ionic sulfonated salts, SDBS or AMPS, can also neutralize surface positive charge in acid media; however, a very large amount of these sulfonated salts (more than 1000 g/t) has to be used and the flocculation performance is still not as good as 10 g/t MMT in the PAM system (results not shown here). Considering the magnitude of the zeta potentials (11.04 mV) of the quartz suspension was not a characteristic of a highly stable system; the surface modification upon MMT adsorption and its interaction with PAM could be the dominant contribution for a better flocculation efficiency.

The PAM molecule was nonionic and linear, and bridging flocculation by PAM for the quartz suspension was generally driven via hydrogen bonds formed between the PAM's amide oxygen and quartz surface silanol groups. Due to the low binding energy, they could not stand the high shear rates such that PAM molecules detached from quartz particles. Once broken, these bonds may not be able to be reformed, so the broken quartz flocs could no longer be held together. Compared to the adsorption energy of PAM on the (101) face of quartz crystalline (-16.93 kJ/mol), the adsorption energy of PAM on the (001) face of MMT crystalline (O-Si-O tetrahedral sheets) is -49.16 kJ/mol [30]. Therefore, the interaction of MMT-modified quartz surface with PAM was greatly enhanced. Sedimentation tests carried out for the 1.0 wt.% 2000-mesh MMT suspension using PAM as flocculants is shown in Figure 12. It can be seen that the MMT suspension was easily flocculated with a much faster settling rate and much lower supernatant turbidity, in comparison with quartz under the same condition. Therefore, the improved flocculation behavior of the MMT addition to the PAM system was due to the stronger hydrogen binding between MMT and PAM than that of quartz and PAM, together with electrostatic attraction between MMT and quartz. Adding SDBS/AMPS can also lead to their adsorption on a quartz surface; however, the van der Waals force existing between these organic small molecules and PAM was much weaker than MMT's hydrogen binding.

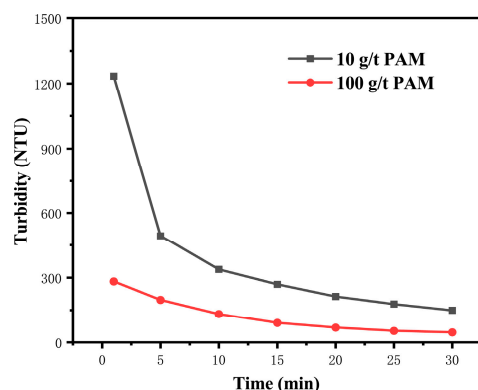


Figure 12. Supernatant turbidity of 1 wt.% -2000-mesh montmorillonite slurry during a 30-min sedimentation.

The synergistic function of the PEO-TA system can be different from that of the PAM-MMT system. The PEO itself behaved better than the PAM because of the stronger hydrogen bonding of PEO's ether oxygen with the silanol-bearing surface [31–33]. The PAM has a higher molecule weight than the PEO, possibly associated with higher viscosity. In this work, adsorption is a more determining factor, compared to molecule weight, in the process of fine silica particle flocculation. The TA had a negligible affinity for quartz, and in such circumstances, previous research has proven that TA barely adsorbed on quartz [27]. It was proposed in the literature that TA interacted with PEO to form associative polymer complexes which then adsorbed onto a mineral surface through PEO [15,16]. Polymeric flocculant dissolved in aqueous solution has a measurable particle size due to molecule structure conformation. Figure 13 shows the molecule size of flocculants measured by dynamic light scattering. It is seen that the formed PEO-TA complexes were larger in size compared to PEO alone, and such a complex structure was more efficient to increase the floc size. In addition, the PEO-TA complexes were comparable with PAM in size, indicating that the formed complexes might have a molecule weight of around 10~12 millions.

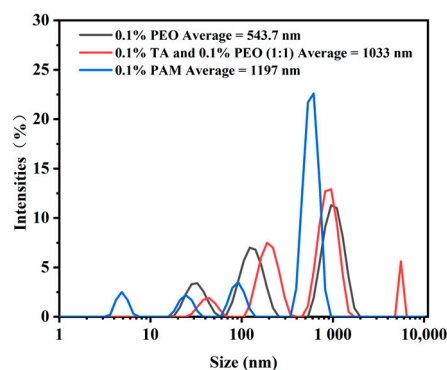


Figure 13. Dynamic Light Scattering measurement: PEO, TA-PEO, and PAM.

The bridging and sweeping between quartz particles can be further promoted by a higher molecule weight flocculant, thus promoting flocculation. A similar conclusion was made in the previous publication for a quartz suspension, particularly in neutral and alkaline suspensions [27]. The present work expanded the application of PEO-TA complexes to more acidic media that could be helpful for acid leaching pulp. It was also proposed that phenolic compounds can increase the stiffness of PEO molecule chains and make them adsorb more easily onto fine particles [16]. Regarding the structure of the TA-PEO associative complex, the initially flexible linear PEO chains may become rigid due to their association with TA. Complexes consisting of well-dissolved PEO entanglements clustered by cofactors ensure the large size of the complexes. As can be seen from Figure 11,

quartz has a low charge density; therefore, its affinity is strong for neutral polymers such as PEO, resulting in adsorption with more trains and loops [34]. The result was that these complex molecules were bonded more firmly with quartz particles (or less likely to desorb), developing large flocs that were more resistant against shear force. The mechanisms underlying the synergistic function of a flocculants/cofactors dual reagents system in quartz flocculation were schematically illustrated in Figure 14.

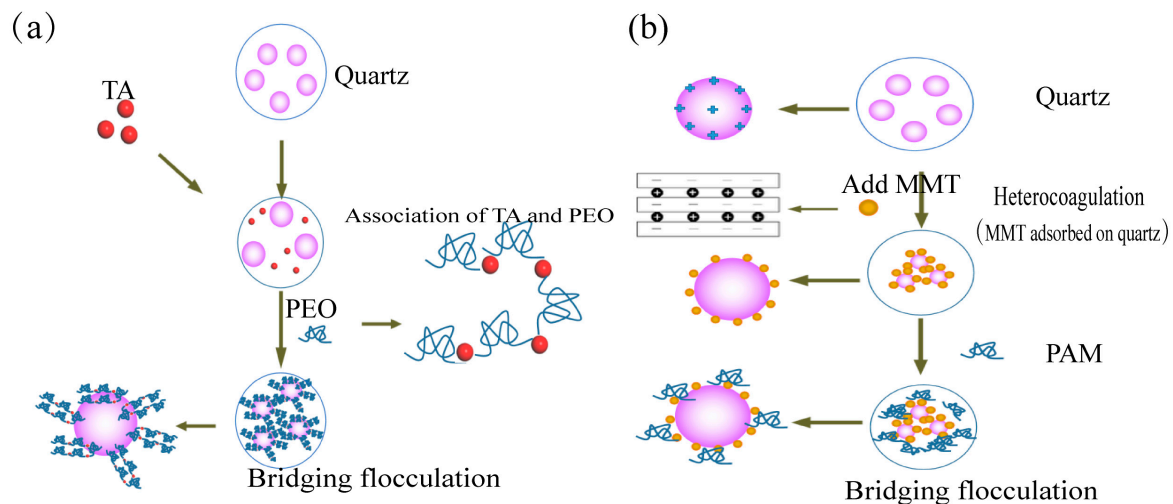


Figure 14. Schematic illustration of flocculation: (a) Quartz-TA-PEO; (b) Quartz-MMT-PAM.

4. Conclusions

The flocculation behaviors of quartz in simulated acid leaching pulp using nonionic flocculant poly(ethylene oxide) (PEO) with a combination of tannic acid (TA) as the cofactor and another combination of nonionic polyacrylamide (PAM) and a negatively charged montmorillonite (MMT) nanosheet were investigated in this study, with dynamic floc size monitoring using the in situ focused beam reflectance measurement technique.

In terms of polymeric flocculants, PEO outperforms PAM by lowering the turbidity of the suspension after flocculation sedimentation, because of the stronger affinity to quartz by the hydrogen bond between the ether oxygen and silanol group. The addition of TA significantly improves the flocculation efficiency of quartz by PEO, and MMT improves the flocculation efficiency by PAM. Flocs breakage upon turbulent conditions plays an important role in the flocculation performance. The higher shear resistance provided by PEO/PEO + TA/PAM + MMT leads to a more compact floc structure with less reduction in floc size and less release of fines upon shear force and, subsequently, clearer suspension upon sedimentation.

However, mechanisms underlying the increase of floc strength by cofactors between TA and MMT can be different in the combinations of PEO + TA and PAM + MMT, respectively. Dynamic light scattering and adsorption measurements confirm that the pathway of the PEO + TA flocculation is via the initial formation of associative complexes between tannic acid and PEO in a solution with the formation of entangled and large-sized clusters, and then bridging of quartz particles by the associative complexes more effectively. The zeta potential measurement and molecule simulation indicate that the pathway of the PAM + MMT flocculation is via MMT nanosheet adsorption on quartz by electrostatic forces, and then bridging of the surface-modified quartz particles more effectively by PAM, due to the more negative adsorption energy of the acrylamino group on tetrahedral sheets. Coagulation might not play a dominant role in PAM + MMT flocculation; although, neutralization of positively charged quartz by a negatively charged MMT nanosheet occurs to some extent. Furthermore, reformation of broken flocs was difficult for both flocculation systems.

Author Contributions: Conceptualization, B.G. and K.J.; methodology, X.Z. and B.G.; software, X.Z.; validation, H.X., R.D. and X.Z.; formal analysis, B.G.; investigation, B.G. and K.J.; resources, B.G. and K.J.; data curation, X.Z.; writing—original draft preparation, X.Z.; writing—review and editing, X.Z. and B.G.; visualization, X.Z. and B.G.; supervision, B.G. and K.J.; project administration, B.G. and H.X.; funding acquisition, H.X. and B.G. All authors have read and agreed to the published version of the manuscript.

Funding: This work is supported by the National Key Research and Development Program (No. 2022YFC2904604) from the Ministry of Science and Technology of China.

Data Availability Statement: Data are available upon reasonable, by the corresponding authors.

Acknowledgments: The SNF was kindly acknowledged for providing flocculants samples.

Conflicts of Interest: The authors declare no conflict of interest.

References

1. Havlik, T. *Hydrometallurgy: Principles and Applications*; Woodward Publishing: Cambridge, UK, 2014.
2. Kazadi, D.M.; Groot, D.R.; Steenkamp, J.D.; Pöllmann, H. Control of silica polymerisation during ferromanganese slag sulphuric acid digestion and water leaching. *Hydrometallurgy* **2016**, *166*, 214–221. [[CrossRef](#)]
3. Ritcey, G.M. Crud in solvent extraction processing—A review of causes and treatment. *Hydrometallurgy* **1980**, *5*, 97–107. [[CrossRef](#)]
4. Fletcher, A.W.; Gage, R.C. Dealing with a siliceous crud problem in solvent extraction. *Hydrometallurgy* **1985**, *15*, 5–9. [[CrossRef](#)]
5. Kitchener, J.A. Principles of action of polymeric flocculants. *Br. Polym. J.* **1972**, *4*, 217–229. [[CrossRef](#)]
6. Lee, C.S.; Robinson, J.; Chong, M.F. A review on application of flocculants in wastewater treatment. *Process Saf. Environ. Prot.* **2014**, *92*, 489–508. [[CrossRef](#)]
7. Hogg, R. Flocculation and dewatering. *Int. J. Miner. Process.* **2000**, *58*, 223–236. [[CrossRef](#)]
8. Moud, A.A. Polymer based flocculants: Review of water purification applications. *J. Water Process Eng.* **2022**, *48*, 102938. [[CrossRef](#)]
9. Loan, M.; Newman, O.M.G.; Cooper, R.M.G.; Farrow, J.B.; Parkinson, G.M. Defining the Paragoethite process for iron removal in zinc hydrometallurgy. *Hydrometallurgy* **2006**, *81*, 104–129. [[CrossRef](#)]
10. Dyer, L.G.; Richmond, W.R.; Fawell, P.D. Simulation of iron oxide/silica precipitation in the paragoethite process for the removal of iron from acidic zinc leach solutions. *Hydrometallurgy* **2012**, *119–120*, 47–54. [[CrossRef](#)]
11. Valenzuela-Elgueta, J.; Delgado, A.V.; Ahualli, S. Effect of cationic surfactant addition on the electrokinetics and stability of silica/kaolinite suspensions in copper hydrometallurgy conditions. *Miner. Eng.* **2021**, *169*, 106958. [[CrossRef](#)]
12. Figdore, P.E. Adsorption of surfactants on kaolinite: NaCl versus CaCl₂ salt effects. *J. Colloid Interface Sci.* **1982**, *87*, 500–517. [[CrossRef](#)]
13. Besra, L.; Sengupta, D.K.; Roy, S.K.; Ay, P. Flocculation and dewatering of kaolin suspensions in the presence of polyacrylamide and surfactants. *Int. J. Miner. Process.* **2002**, *66*, 203–232. [[CrossRef](#)]
14. Cong, R.; Pelton, R. The influence of PEO/poly(vinyl phenol-co-styrene sulfonate) aqueous complex structure on flocculation. *J. Colloid Interface Sci.* **2003**, *261*, 65–73. [[CrossRef](#)] [[PubMed](#)]
15. Gaudreault, R.; van de Ven, T.G.M.; Whitehead, M.A. Mechanisms of flocculation with poly(ethylene oxide) and novel cofactors. *Colloids Surf. A Physicochem. Eng. Asp.* **2005**, *268*, 131–146. [[CrossRef](#)]
16. van de Ven, T.G.M. Association-induced polymer bridging by poly(ethylene oxide)–cofactor flocculation systems. *Adv. Colloid Interface Sci.* **2005**, *114–115*, 147–157. [[CrossRef](#)] [[PubMed](#)]
17. Zhou, C.; Tong, D.; Yu, W. 7-Smectite Nanomaterials: Preparation, Properties, and Functional Applications. In *Nanomaterials from Clay Minerals*; Wang, A., Wang, W., Eds.; Elsevier: Amsterdam, The Netherlands, 2019; pp. 335–364.
18. Peng, C.; Min, F.; Liu, L. Effect of pH on the adsorption of dodecylamine on montmorillonite: Insights from experiments and molecular dynamics simulations. *Appl. Surf. Sci.* **2017**, *425*, 996–1005. [[CrossRef](#)]
19. Emmerich, K.; Koeniger, F.; Kaden, H.; Thissen, P. Microscopic structure and properties of discrete water layer in Na-exchanged montmorillonite. *J. Colloid Interface Sci.* **2015**, *448*, 24–31. [[CrossRef](#)]
20. Shi, D.; Yu, W.; Li, R.K.Y.; Ke, Z.; Yin, J. An investigation on the dispersion of montmorillonite (MMT) primary particles in PP matrix. *Eur. Polym. J.* **2007**, *43*, 3250–3257. [[CrossRef](#)]
21. Oueslati, W.; Ben Rhaïem, H.; Lanson, B.; Ben Haj Amara, A. Selectivity of Na–montmorillonite in relation with the concentration of bivalent cation (Cu²⁺, Ca²⁺, Ni²⁺) by quantitative analysis of XRD patterns. *Appl. Clay Sci.* **2009**, *43*, 224–227. [[CrossRef](#)]
22. Heath, A.; Fawell, P.; And, P.B.; Swift, J. Estimating Average Particle Size by Focused Beam Reflectance Measurement (FBRM). *Part. Part. Syst. Charact.* **2002**, *19*, 84–95. [[CrossRef](#)]
23. Grabsch, A.F.; Yahyaie, M.; Fawell, P.D. Number-sensitive particle size measurements for monitoring flocculation responses to different grinding conditions. *Miner. Eng.* **2020**, *145*, 106088. [[CrossRef](#)]
24. Kyoda, Y.; Costine, A.D.; Fawell, P.D.; Bellwood, J.; Das, G.K. Using focused beam reflectance measurement (FBRM) to monitor aggregate structures formed in flocculated clay suspensions. *Miner. Eng.* **2019**, *138*, 148–160. [[CrossRef](#)]

25. Spicer, P.T.; Pratsinis, S.E.; Raper, J.; Amal, R.; Bushell, G.; Meesters, G. Effect of shear schedule on particle size, density, and structure during flocculation in stirred tanks. *Powder Technol.* **1998**, *97*, 26–34. [[CrossRef](#)]
26. Wang, C.; Sun, C.; Liu, Q. Formation, breakage, and re-growth of quartz flocs generated by non-ionic high molecular weight polyacrylamide. *Miner. Eng.* **2020**, *157*, 106546. [[CrossRef](#)]
27. Wang, D.; Wang, D.; Deng, C.; Wang, K.; Tan, X.; Liu, Q. Flocculation of quartz by a dual polymer system containing tannic acid and poly(ethylene oxide): Effect of polymer chemistry and hydrodynamic conditions. *Chem. Eng. J.* **2022**, *446*, 137403. [[CrossRef](#)]
28. Owen, A.T.; Fawell, P.D.; Swift, J.D.; Labbett, D.M.; Benn, F.A.; Farrow, J.B. Using turbulent pipe flow to study the factors affecting polymer-bridging flocculation of mineral systems. *Int. J. Miner. Process.* **2008**, *87*, 90–99. [[CrossRef](#)]
29. Swift, J.D.; Simic, K.; Johnston, R.R.M.; Fawell, P.D.; Farrow, J.B. A study of the polymer flocculation reaction in a linear pipe with a focused beam reflectance measurement probe. *Int. J. Miner. Process.* **2004**, *73*, 103–118. [[CrossRef](#)]
30. Huang, Y. *Study on Settlement Mechanism of Fine Kaolinite Tailing Ballasted Flocculation by Quartz Carrier*; China University of Mining and Technology: Beijing, China, 2019.
31. Mporfu, P.; Addai-Mensah, J.; Ralston, J. Flocculation and dewatering behaviour of smectite dispersions: Effect of polymer structure type. *Miner. Eng.* **2004**, *17*, 411–423. [[CrossRef](#)]
32. Mporfu, P.; Addai-Mensah, J.; Ralston, J. Investigation of the effect of polymer structure type on flocculation, rheology and dewatering behaviour of kaolinite dispersions. *Int. J. Miner. Process.* **2003**, *71*, 247–268. [[CrossRef](#)]
33. Rubio, J.; Kitchener, J.A. The mechanism of adsorption of poly(ethylene oxide) flocculant on silica. *J. Colloid Interface Sci.* **1976**, *57*, 132–142. [[CrossRef](#)]
34. Quezada, G.R.; Piceros, E.; Saavedra, J.H.; Robles, P.; Jeldres, R.I. Polymer affinity with quartz (101) surface in saline solutions: A molecular dynamics study. *Miner. Eng.* **2022**, *186*, 107750. [[CrossRef](#)]

Disclaimer/Publisher’s Note: The statements, opinions and data contained in all publications are solely those of the individual author(s) and contributor(s) and not of MDPI and/or the editor(s). MDPI and/or the editor(s) disclaim responsibility for any injury to people or property resulting from any ideas, methods, instructions or products referred to in the content.